PHEMT saturation velocity and mobility is taken 1.5×10^7 cm/sec and 7000 $cm^2/V \cdot sec$, respectively.

CONCLUSION

An analytical noise modeling is performed using an accurate charge-control model to evaluate the small-signal parameters and noise properties of HEMT and PHEMT. This model shows improved behavior of transconductance and gate-to-source capacitance near the threshold region; hence, the calculated curves of minimum noise figure F_{min} and minimum noise temperature T_{min} show good matching with the experimental data. Excellent agreement with the experimental results ensures the validity of the proposed model. The effects of gate length and donor layer thickness upon noise performance are also studied, which suggest that noise performance improves with reducing gate length and increasing thickness, however, one needs to maintain the aspect ratio in order to avoid short-channel effects.

ACKNOWLEDGMENT

The authors would like to thank the Defense Research and Development Organization, Ministry of Defense, Govt. of India, for financial support.

REFERENCES

1. K.H.G. Duh, M.W. Pospieszalski, W.F. Kopp, P. Ho, A.A. Jabra, P.C. Chao, P.M. Smith, L.F. Lester, J.M. Ballingall, and S. Weinreb, Ultra-low-noise cryogenic high electron mobility transistors, IEEE Trans Electron Devices 35 (1988), 249–254.
2. K.H.G. Duh, S.M. Liu, L.F. Lester, P.C. Chao, P.M. Smith, M.B. Das, B.R. Lee, and J. Ballingall, Ultra-low-noise characteristics of millimeter-wave high electron mobility transistors, IEEE Electron Devices Lett 9 (1988), 521–523.
3. K.L. Tan, R.M. Dia, D.C. Streit, T. Lin, T.Q. Trinh, A.C. Han, P.H. Liu, P.D. Chow, and H.C. Yen, 94-GHz 0.1-μm T-gate low-noise pseudomorphic InGaAs HEMTs, IEEE Electron Device Lett 11 (1990), 585–587.
4. K.L. Tan, R.M. Dia, D.C. Streit, L.K. Shaw, A.C. Han, M.D. Sholley, P.H. Liu, T.Q. Trinh, T. Lin, and H.C. Yen, 60-GHz pseudomorphic $Al_{0.25}Ga_{0.75}As/In_{0.28}Ga_{0.72}As$ low-noise HEMTs, IEEE Electron Device Lett 12 (1991), 23–25.
5. J. Lee, H. Yoon, C. Park, and H. Park, Ultra-low-noise characteristics of AlGaAs/InGaAs/GaAs pseudomorphic HEMTs with wide-head T-shaped gate, IEEE Electron Device Lett 16 (1995), 271–273.
6. T. Hwang, P. Chye, and P. Gregory, Super low-noise pseudomorphic InGaAs channel InP HEMTs, Electron Lett 29 (1993), 10–11.
7. N. Yoshida, T. Kitano, Y. Yamamoto, T. Katoh, H. Minami, T. Kashiwa, et al., Super low-noise InAlAs/InGaAs HEMT processed by selective wet gate recess etching, IEEE Trans Electron Devices 43 (1996), 178–180.
8. R.A. Pucel, H.A. Haus, and H. Statz, Advances in electronics and electron physics, Academic Press, New York, 1975, pp 195–265.
9. M.W. Pospieszalski, Modelling of noise parameters of MESFET's and MODFET's and their frequency and temperature dependence, IEEE Trans Microwave Theory Tech 37 (1989), 1340–1350.
10. T.M. Brooks, The noise properties of high electron mobility transistors, IEEE Trans Electron Devices 33 (1986), 52–57.
11. Y. Ando and T. Itoh, DC, small signal, and noise modeling for two-dimensional electron gas field effect transistors based on accurate charge control characteristics, IEEE Trans Electron Devices 37 (1990), 67–78.
12. A.F.M. Anwer and K.W. Liu, A noise model for high electron mobility transistors, IEEE Trans Electron Devices 41 (1994), 2087–2092.
13. N. Dasgupta and A. Dasgupta, An analytical expression for sheet carrier concentration vs. gate voltage for HEMT modeling, Solid State electronics, 36 (1993), 201–203.
14. V. Guru, H.P. Vyas, M. Gupta, and R.S. Gupta, Analytical noise model of a high-electron-mobility transistor for microwave-frequency application, Microwave Opt Technol Lett 40 (2004), 410–417.
15. K. Kamei, Extremaly low-noise 0.25-μm gate HEMTs, Proc 12th GaAs Related Compounds Conf, 1985, pp 541–546.
16. J. Wenger, Quarter-micrometer low-noise pseudomorphic GaAs HEMTs with extremaly low dependence of the noise figure on drain-source current, IEEE Electron Devices Lett 14 (1993), 16–18.
17. R. Plana, L. Escoutte, O. Llopis, H. Amine, T. Parra, M. Gayral, and J. Graffeuil, Noise in AlGaAs/InGaAs/GaAs pseudomorphic HEMTs from 10 Hz to 18 GHz, IEEE Trans Electron Devices 40 (1993), 852–859.
18. T. Hwang, T.M. Kao, D. Glajchen, and P. Chye, Pseudomorphic AlGaAs/InGaAs/GaAs HEMTs in low-cost plastic packaging for DBS application, Electron Lett 32 (1996), 141–143.
19. K. Joshin, Y. Mimino, S. Ohmura, and Y. Hirachi, Noise performance at cryogenic temperatures of AlGaAs/InGaAs HEMT's with 0.15-μm-T-shaped W Si_x gates, IEEE Trans Electron Devices 39 (1992), 515–519.

OPTIMUM COMPACT H- AND E-PLANE CORNERS IN RECTANGULAR WAVEGUIDE

Alicia Casanueva, José A. Pereda, and Angél Mediavilla
Departamento de Ingeniería de Comunicaciones (DICOM)
Universidad de Cantabria
Avda. Los Castros s/n
39005 Santander, Spain

Received 23 February 2004

ABSTRACT: *H- and E-plane corners in rectangular waveguide are widely used in microwave systems. An important aspect in the design of these components is to maintain a specified return loss over a wide-frequency band. Designs that are compact in size are also required to fulfill space and insertion-loss restrictions. In this paper, two families of compact matched corners are considered: the multistepped and multimitered compact matched corners. Optimum physical dimensions that minimize return losses over the full-frequency band are given for the first three members of each family, for the H- and E-plane cases. In addition, a yield analysis of the optimum structures is included. The results are obtained by using the electromagnetic commercial simulator μWave Wizard.* © 2004 Wiley Periodicals, Inc. Microwave Opt Technol Lett 42: 494–497, 2004; Published online in Wiley InterScience (www.interscience.wiley.com). DOI 10.1002/mop.20347

Key words: *H- and E-plane corners; rectangular waveguide; electromagnetic simulation; yield analysis*

1. INTRODUCTION

H- and E-plane corners in rectangular waveguide are intensively used in most microwave systems. A major aspect in the design of waveguide corners is to maintain a specified return loss over a wide bandwidth, for instance, −35 dB usually gives a desirable performance in scientific and industrial applications such as antenna subsystems [1]. Additionally, space and insertion loss restrictions call for designs that are compact in size.

In the past, waveguide corners were analyzed experimentally and equivalent circuits were proposed to model their electromagnetic behavior [2]. During the last decade, several rigorous numerical methods for the analysis and optimization of these elements have been proposed [3–6]. However, these publications mainly focus on the numerical methods themselves and, from our view-

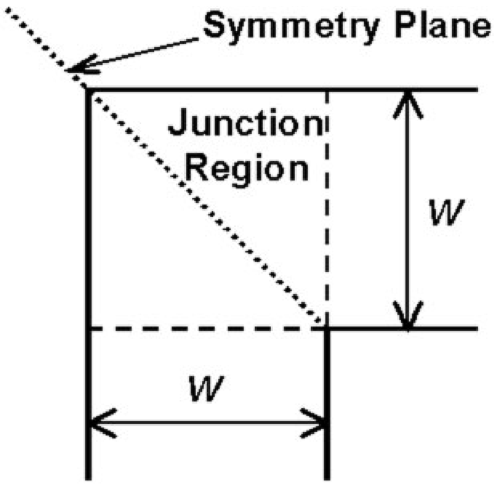

Figure 1 Unmatched waveguide corners in rectangular waveguide. For the H-plane case, w represents the waveguide with ($w = a$), while for the E-plane case it represents the waveguide height ($w = b$)

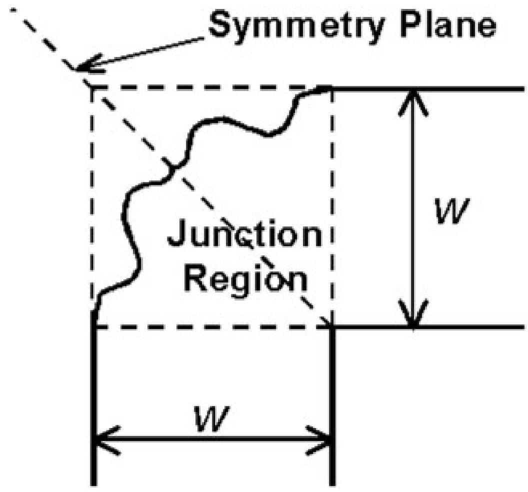

Figure 3 General compact matched corner

point, a systematic study of compact H- and E-plane matched corners has not been given yet.

The aim of this contribution is to fill this gap. To this end, a general topology for compact corners is introduced and two particular realizations of this topology are considered: the multistepped and the multimitered corners. In fact, each particular realization is a family of corners. The first three members of each family are considered in this study and optimum physical dimensions for the H- and E-plane cases are given. Moreover, a yield analysis of the optimum structures is also included. Electromagnetic simulations are carried out by using the commercial simulator μWave Wizard [7].

2. ANALYSIS AND OPTIMIZATION

As a starting point, we consider the analysis of the unmatched H- and E-plane waveguide corners shown in Figure 1. These structures can be considered as two orthogonal waveguide arms of the same size, $a \times b$, connected by a junction region. These structures are thus symmetric with respect to the plane shown in Figure 1. Figure 2 shows the return loss for the H- and E-plane unmatched corners in WR75 waveguide ($a = 19.05$ mm, $b = a/2$). It can be seen that both corners are highly unmatched and they exhibit a very dispersive response which resembles the response of a cavity rather than that of a transition. In fact, these structures are also used as waveguide-filter sections.

The goal is now to improve the return loss of the corners shown in figure 1 without increasing their physical size. To this end, we consider a general compact matched corner shown in Figure 3. The basic idea behind this structure is to reduce the volume of the junction region in order to provide a smooth transition between the two orthogonal waveguide arms while maintaining the symmetry plane. A first-sight matched corner, falling within this category, could be the rounded corner (see the inset of Fig. 4). The return loss for the H- and E-plane versions of this structure is depicted in Figure 4. For both planes the matching is improved; however, the worst-case return loss in the band is not good enough, since it is still far from the initial goal of -35 dB. Moreover, the rounded corner has no free parameters and, consequently, it does not allow the response to be optimized. A possible generalization of this structure consists of rounding the interior corner as well [8]. In such a case, however, the size of the junction region increases and the compactness of the structure is lost.

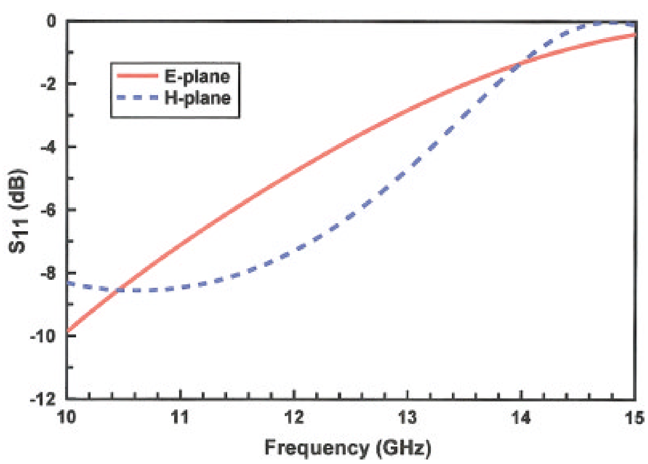

Figure 2 Return loss for unmatched H- and E-plane waveguide corners. [Color figure can be viewed in the online issue, which is available at www.interscience.wiley.com]

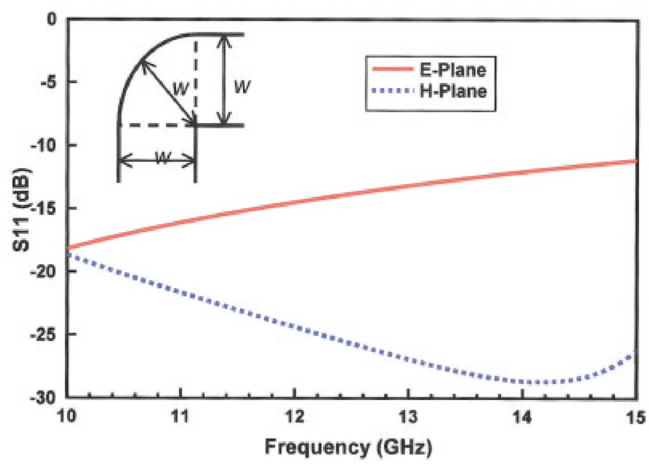

Figure 4 Return loss for rounded H- and E-plane corners. [Color figure can be viewed in the online issue, which is available at www.interscience.wiley.com]

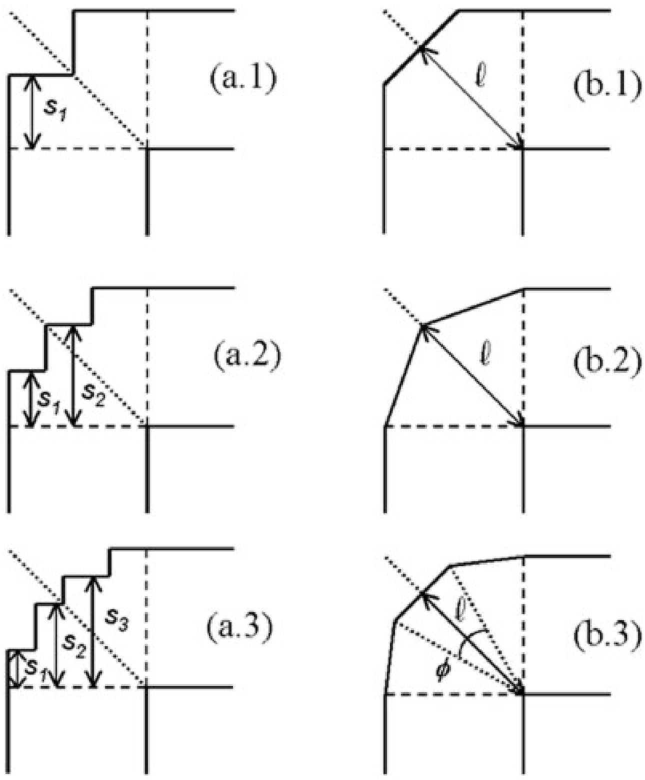

Figure 5 Multistepped and multimitered compact matched corners

As a practical realization of the general compact matched corner shown in Figure 3, we consider two families of structures. We will refer to them as the multistepped and multimitered compact matched corners. The first three members of each family are depicted in Figure 5.

Figure 6 plots the return loss for the first three multistepped H-plane corners. The dimensions of these structures have been optimized to minimize return loss over the whole frequency band (10–15 GHz) of the standard WR75 waveguide. The shape of the optimized responses shows that the single-stepped corner has a resonance into the band and the double-stepped corner has two resonances. It can be seen, however, that for a larger number of steps in the junction region, the number of resonances does not increase, it is also two. It can be seen that the matching improves as the number of steps increases.

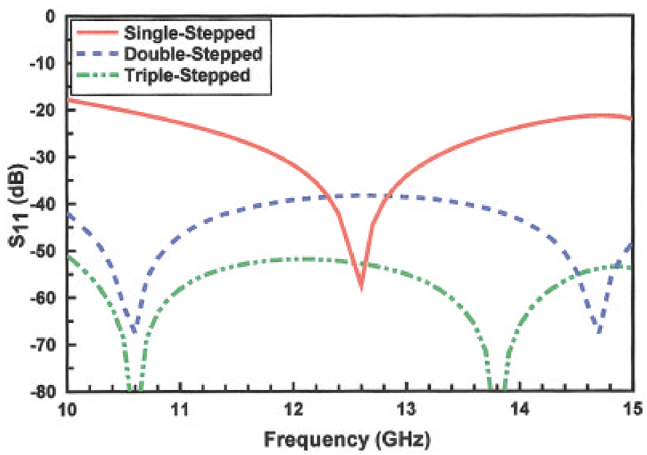

Figure 6 Return loss for the first three multistepped H-plane corners. [Color figure can be viewed in the online issue, which is available at www.interscience.wiley.com]

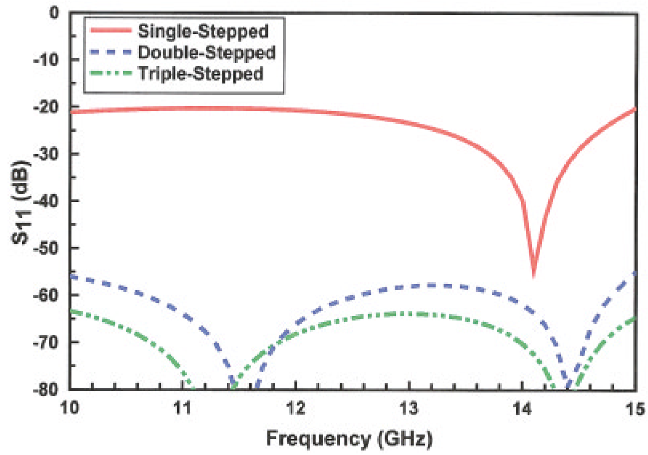

Figure 7 Return loss for the first three multistepped E-plane corners. [Color figure can be viewed in the online issue, which is available at www.interscience.wiley.com]

In Figure 7, the return loss for the first three multistepped E-plane corners is plotted. The same comments as for the H-plane case can be repeated here. Comparing these results with those in Figure 6 we observe that, for the same number of steps, the E-plane corner gives better performance than its H-plane counterpart.

Figure 8 shows the return loss for the first three multimitered H-plane corners. As in Figures 6 and 7, the dimensions of these structures have been optimized in order to minimize the return loss over the whole band. However, note that in this case, the double-mitered corner has only one physical parameter to be optimized (as the single-mitered corner), and the triple-mitered corner has two parameters, the angle ϕ and the length ℓ. In fact, it can be observed in Figure 8 that both the single- and double-mitered corners have only one resonance into the band, while the triple-mitered structure has two resonances.

In Figure 9, the optimum return loss for the first three multimitered E-plane corners is plotted. In all three cases, only one resonance was found in the band.

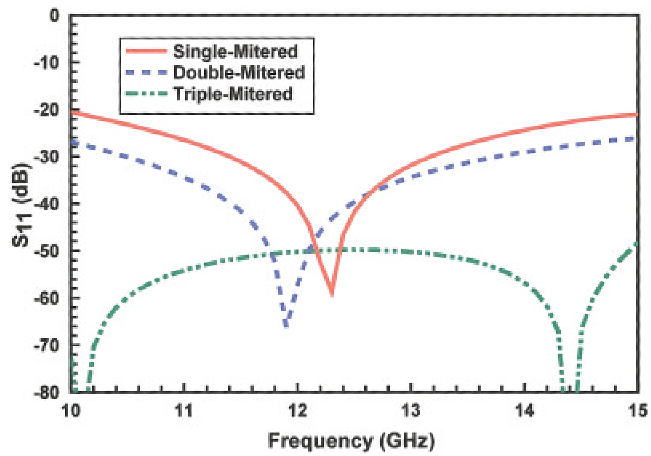

Figure 8 Return loss for the first three multimitered H-plane corners. [Color figure can be viewed in the online issue, which is available at www.interscience.wiley.com]

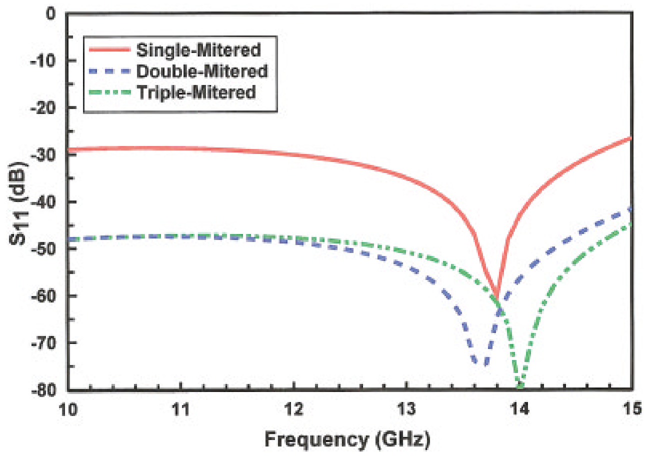

Figure 9 Return loss for the first three multimitered E-plane corners. [Color figure can be viewed in the online issue, which is available at www.interscience.wiley.com]

TABLE 1 Optimum Dimensions and Worst-Case Return Loss for H-Plane Corners

Stepped Corners	s_1/a	s_2/a	s_3/a	$\|S_{11}\|$ (dB)
Single-stepped	0.64	—	—	−18
Double-stepped	0.37	0.80	—	−38
Triple-stepped	0.26	0.63	0.87	−51
Mitered Corners	ℓ/a	ϕ	—	$\|S_{11}\|$ (dB)
Single-mitered	0.96	—	—	−20
Double-mitered	0.96	—	—	−26
Triple-mitered	0.92	30.6°	—	−48

TABLE 2 Optimum Dimensions and Worst-Case Return Loss for E-Plane Corners

Stepped Corners	s_1/b	s_2/b	s_3/b	$\|S_{11}\|$ (dB)
Single-stepped	0.53	—	—	−20
Double-stepped	0.23	0.74	—	−55
Triple-stepped	0.20	0.61	0.77	−63
Mitered Corners	ℓ/b	ϕ	—	$\|S_{11}\|$ (dB)
Single-mitered	0.86	—	—	−27
Double-mitered	0.91	—	—	−42
Triple-mitered	0.87	29.7°	—	−47

Optimum physical dimensions and the corresponding worst-case return loss for the structures shown in Figure 5 are summarized in Tables 1 and 2. To provide an easy way of scaling the dimensions to other frequency bands, the dimensions for H-plane corners have been normalized to the waveguide width a, while for the E-plane case they have been normalized to the waveguide height b.

3. YIELD VALIDATION

In order to determine the manufacturability of the optimum designs presented above, a yield analysis using both Gaussian and Uniform distribution has been performed. In all the cases, the geometry tolerance was set to a standard value of ± 0.05 mm, which can be easily reached for any milling machine.

Table 3 shows, for the abovementioned geometrical tolerance, the worst-case values for the return loss inside the considered frequency band (10–15 GHz). As expected, geometrical tolerances mainly affects the cases where return losses are very low, that is, double- and triple-stepped/mitered corners.

TABLE 3 Yield Analysis for the Optimum H- and E-Plane Corners Whose Nominal Dimensions are Given in Tables 1 and 2

	Worst-Case $\|S_{11}\|$ (dB)	
Corner	(H-Plane)	(E-Plane)
Single-stepped	−17.5	−19.5
Double-stepped	−37	−42
Triple-stepped	−45	−44
Single-mitered	−19.5	−26.5
Double-mitered	−25.5	−38
Triple-mitered	−46	−42

4. CONCLUSION

A general topology for compact matched corners in rectangular waveguide has been introduced and two practical realizations of this topology—the multistepped and the multimitered corners—have been studied. The first three members of each family have been considered in this study and optimum physical dimensions, for the H- and E-plane cases, have been given.

In general, the E-plane matched corners analyzed give better results than their H-plane counterpart.

The double-stepped/mitered realizations provide nominal worst-case return loss, in the whole frequency band, that is better than −35 dB (except the H-plane double-mitered corner which gives only −26 dB).

The yield analysis performed shows that double- and triple-stepped/mitered realizations give similar worst-case return losses, which are good enough for most applications. Specifically, the double-stepped corner is a simple structure that provides good enough matching with relatively small sensibility to mechanical tolerances.

5. ACKNOWLEDGMENT

The authors wish to thank Dr. T. Sieverding for his useful suggestions and help with the software.

REFERENCES

1. J. Uher, J. Bornemann, and U. Rosenberg, Waveguide components for antenna feed systems: Theory and CAD, Artech House, Norwood, MA, 1993, ch. 3.
2. N. Marcuvitz, Waveguide handbook, McGraw-Hill, New York, 1953.
3. K.L. Wu, G.Y. Delisle, D.G. Fang, and M. Lecours, Waveguide discontinuity analysis with a coupled finite-boundary element method, IEEE Trans Microwave Theory Tech MTT-37 (1989), 993–998.
4. J.M. Rieter and F. Arndt, A full-wave boundary contour mode-matching method (BCMM) for the rigorous CAD of single and cascaded optimized H-plane and E-plane bends, Proc IEEE MTT-S Dig, San Diego, CA, (1994), 1021–1024.
5. F. Alessandri, M. Mongiardo, and R. Sorrentino, Rigorous mode-matching analysis of mitered E-plane bends in rectangular waveguide, IEEE Microwave Guided Wave Lett MGWL-4 (1994), 408–410.
6. V.A. Labay and J. Bornemann, Generalized scattering matrix of waveguide corners distorted by discontinuities in the resonator region, Proc IEEE MTT-S Dig, Orlando, FL, (1995), 269–272.
7. μWave Wizard software, http://www.mician.com.
8. M. Mongiardo, A. Morini, and T. Rozzi, Analysis and design of full-band matched waveguide bends, IEEE Trans Microwave Theory Tech MTT-43 (1995), 2965–2971.